# Schwann cell-derived exosomes induce bone marrow-derived mesenchymal stem cells to express Schwann cell markers *in vitro*

HUI WANG[1], YANJUN JIA[2], JIAMOU LI[3] and QINGSONG LIU[1]

[1]Department of Otolaryngology Head and Neck Surgery, Beijing Luhe Hospital, Capital Medical University, Beijing 101199; [2]Medical Research Center, Beijing Chaoyang Hospital, Capital Medical University, Beijing 100043; [3]Department of Orthopedics, Beijing Tiantan Hospital, Capital Medical University, Beijing 100070, P.R. China

Received January 16, 2019; Accepted November 27, 2019

DOI: 10.3892/mmr.2020.10960

**Abstract.** Following peripheral nerve injury, factors in the local microenvironment can induce the differentiation of bone marrow-derived mesenchymal stem cells (BMSCs) into Schwann cells; however, the specific factors that participate in this process remain unclear. The present study aimed to investigate the role of Schwann cell-derived exosomes in the differentiation of BMSCs into Schwann cells. Exosomes were extracted from Schwann cells or fibroblasts and co-cultured with BMSCs. The morphology, as well as gene and protein expressions of the BMSCs were measured to determine the effect of exosomes on cell differentiation. The levels of Schwann cell-specific markers in BMSCs were significantly increased by Schwann cell-derived exosomes compared with untreated BMSCs; however, fibroblast-derived exosomes did not demonstrate the same effects. In conclusion, Schwann cell-derived exosomes may be involved in the differentiation of BMSCs into Schwann cells, which may provide a novel target for promoting nerve regeneration following injury.

## Introduction

Bone marrow-derived mesenchymal stem cells (BMSCs) can differentiate into Schwann cells (key factors for nerve regeneration) under different conditions, such as during sciatic nerve transection and nerve regeneration chamber to promote the regeneration of damaged nerves (1-4). BMSCs transplanted *in vivo* to damaged areas can differentiate into the corresponding Schwann cells (1,2,4-6), which suggested that following injury, multiple factors may be produced in the local *in vivo* microenvironment that can induce BMSCs to differentiate into Schwann cells to repair the injured tissue; however, the factors involved in this process are unclear.

Exosomes are small cell-derived vesicles that commonly are found in human body fluids, including blood, urine and tissue fluids (7,8). Exosomes serve different functions in the body, including participating in intercellular signaling transduction, cell waste secretion and cell fusion (8). Following nerve injury, Wallerian degeneration and Schwann cell proliferation occurs at the distal end of the nerve, forming a regenerative Büngner zone that promotes and guides proximal nerve regeneration (9). During this process, exosomes secreted by Schwann cells promote the regeneration of peripheral nerves and guide the direction of growth of regenerating axons (10,11); thus, there are large numbers of exosomes in the microenvironment following injury, which serve an important role in the recovery of nerve damage. In addition, previous studies have demonstrated that BMSCs participate in the myelination of spinal axons after being cultured with rat dorsal root ganglion cells, and Schwann cell co-culture can induce BMSCs to differentiate into Schwann cells (12-14). These studies suggest that during nerve regeneration within the microenvironment, in which Schwann cells are present, certain factors can induce BMSCs to differentiate into Schwann cells and participate in axonal regeneration. Due to exosomes being involved in the repair of nerve damage, it was hypothesized that exosomes may also have an important role in stem cell differentiation following injury. In the present study, the effect of Schwann cell-derived exosomes on the differentiation of BMSCs into Schwann cells was investigated.

## Materials and methods

*Animal studies*. All animal procedures were conducted in accordance with The Guidelines for Ethical Conduct in the Care and Use of Animals of the Chinese National Health and Medical Research Council, and were approved by the Animal Experimentation Ethics Committee of Capital Medical College (Beijing, China; protocol no. AEEI-2016-135).

*BMSC culture and differentiation into Schwann cells*. Rat BMSCs were obtained from the bone marrow of one eight-week-old male Wistar rat, which weighed between 230-270 g, as previously described (3,15). The rat was housed

*Correspondence to:* Dr Hui Wang, Department of Otolaryngology Head and Neck Surgery, Beijing Luhe Hospital, Capital Medical University, 82 Xinhuananlu, Tongzhou, Beijing 101199, P.R. China
E-mail: whtelzntel@163.com

*Key words:* bone marrow-derived mesenchymal stem cells, Schwann cells, exosomes, differentiation

in a pathogen-free climate-controlled facility with food and water available *ad libitum*. BMSCs were cultured in α-MEM growth media (HyClone; GE Healthcare Life Sciences) supplemented with 10% FBS (Gibco; Thermo Fisher Scientific, Inc.). The third passage of cells was used for subsequent experiments. Rat Schwann cells (RSC96) and fibroblasts were purchased from Shanghai Fuxiang Company (www.xiangbio.com/timemodel/product/2010-03-08/8421285.html). BMSCs were subsequently divided into three experimental groups: i) BMSCs induced to differentiate into Schwann cells using the Dezawa's induction method, as previously described (3); ii) BMSCs induced to differentiate into Schwann cells by Schwann cell-derived exosomes, in which BMSCs were cultured and passaged for 7 days prior to the addition of 200 $\mu$g Schwann cell-derived exosomes to the media (the media was changed every 3 days, with the exosomes being replenished each time); iii) BMSCs induced to differentiate into Schwann cells by fibroblast-derived exosomes, in which BMSCs were cultured and passaged for 7 days prior to the addition of 200 $\mu$g fibroblast-derived exosomes to the media (the media was changed every 3 days, with the exosomes being replenished each time). RSC96 cells were used as the positive control group, and untreated BMSCs were used as the negative control group. A preliminary study was conducted to predetermine the dosage of Schwann cell-derived exosomes required to induce BMSCs; out of 50, 100 or 200 $\mu$g, 200 $\mu$g in 10 ml culture media induced fusiform shape change, in BMSCs. Therefore, the present study used 200 $\mu$g exosomes for the induction of BMSCs (Fig. S1).

*Exosome extraction, identification and quantification*. Exosomes were extracted from fibroblasts (fb exo) and RSC96 (RSC96 exo) cells using the ExoQuick-TC kit (System Biosciences, LLC). The culture media containing the BMSCs was centrifuged (3,000 x g; 15 min; 4˚C) to remove apoptotic cells and cell debris. A total of 3.3 ml exosome precipitation solution was added to 10 ml culture supernatant and incubated at 4˚C overnight. The mixture was centrifuged (10,000 x g; 30 min; 4˚C) and the supernatant was discarded. The isolated exosomes were re-suspended in PBS and the protein concentration was quantified using a bicinchoninic assay kit. Briefly, the standards were diluted to different concentrations (0, 0.2, 0.4, 0.6, 0.8 or 1.0 $\mu$g/$\mu$l). The samples and standards were loaded separately and incubated with the working solution for 30 min at 37˚C in the dark. The optical density values were measured using a microplate reader and the sample concentration was determined according to the standard curve generated. The amount of culture medium and exosomes required was calculated to a final concentration of 20 $\mu$g/ml and used in the subsequent experiments. CD63, CD81 and calnexin were detected by western blotting to confirm the isolation of exosomes.

*Transmission electron microscopy (TEM) of exosomes*. A total volume of 50 $\mu$l exosomes were plated onto red wax. The polyvinyl acetate/carbon-coated copper mesh was placed in the droplets and allowed to stand at room temperature for 20 min. The copper mesh was fixed with 2% paraformaldehyde for 2 min at room temperature, washed three times with double-distilled $H_2O$, and counterstained with 2% phosphotungstic acid (XiYa Reagent; http://m.xiyashiji.com/product/info/id/4724.html) for 1 min at room temperature. Filter paper was used to remove excess liquid from the copper mesh, which was subsequently dried overnight at room temperature. The extracted exosomes were observed using TEM (magnification, x25,000).

*Cellular morphology observation*. After 2, 4 and 7 days of cell differentiation, cellular morphology was observed using a CX41 light microscope (magnification, x200; Olympus Corporation).

*Reverse transcription-quantitative PCR (RT-qPCR)*. Total RNA was extracted from the BMSCs using TRIzol® reagent (cat. no. R0016; Beyotime Institute of Biotechnology) according to the manufacturer's protocol. Total RNA was reverse transcribed into cDNA using the TransScript First-Strand cDNA Synthesis kit (Beijing Transgen Biotech Co., Ltd.). The RT reaction conditions were as follows: 25˚C for 10 min, 42˚C for 30 min, and 85˚C for 5 min. qPCR was subsequently performed using the SYBR® Green Realtime PCR Master mix (Toyobo Life Science; QPK-201) and the ABI PRISM™ 7500 system (Applied Biosystems; Thermo Fisher Scientific, Inc.). The following primer pairs for each marker gene are presented in Table I. The following thermocycling conditions were used for the qPCR: Initial denaturation at 50˚C for 2 min, 94˚C for 2 min, 40 cycles of 94˚C for 5 sec, 60˚C for 30 sec of denaturation, annealing and elongation, 72˚C for 5 min of final extension Expression levels were quantified using the $2^{-\Delta\Delta Cq}$ method (16).

*Western blotting*. Total protein was lysed from cells using lysis buffer (Beijing Solarbio Science & Technology Co., Ltd.) and the lysate was collected using a cell scraper. The lysate was centrifuged (13,523 x g; 5 min; 4˚C) and the supernatant was collected and transferred to a 0.5 ml centrifuge tube. Protein samples were mixed with 5X loading buffer, incubated at 95˚C for 5 min, rapidly cooled on ice and stored at -80˚C until required for further experimentation. Total protein was quantified using a bicinchoninic acid assay kit and 40 $\mu$g protein samples and markers (cat. no. SM1811; Fermentas; Thermo Fisher Scientific, Inc.) were separated via 12% SDS-PAGE. The separated proteins were subsequently transferred onto a nitrocellulose membrane (Merck KGaA) and blocked for 2 h at room temperature with 5% non-fat milk diluted in TBS-Tween-20 (TBST). The membranes were incubated with the following primary antibodies overnight at 4˚C: Anti-Sox10 (1:1,000; cat. no. DF8009; Affinity Biosciences), anti-early growth response 2 (EGR2; 1:500; cat. no. AF0480; Affinity Biosciences), anti-S100 (1:1,000; cat. no. AF0251; Affinity Biosciences), anti-glial fibrillary acidic protein (GFAP; 1:1,000; cat. no. AF6166; Affinity Biosciences), anti-low-affinity nerve growth factor receptor (NGFR; 1:2,000; cat. no. OM267104; Omnimabs), anti-GADPH (1:1,000; cat. no. AB-P-R 001; Hangzhou Goodhere Biotechnology Co., Ltd.), anti-CD63 (1:1,000; cat. no. DF2305; Affinity Biosciences), anti-CD81 (1:1,000; cat. no. DF2306; Affinity Biosciences) and anti-Calnexin (1:1,000; cat. no. AF5362; Affinity Biosciences). Membranes were washed three times (10 min each) with 0.1% TBST at room temperature. Following the primary antibody incubation, membranes were incubated with a horseradish peroxidase-conjugated goat

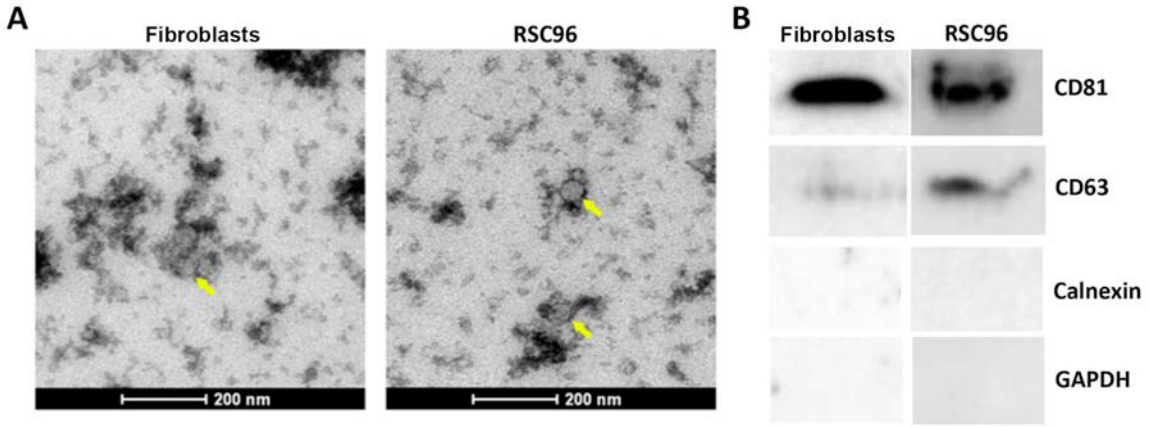


Figure 1. Extraction of exosomes from fibroblasts and RSC96 cells. (A) Transmission electron microscopy images of exosomes (yellow arrows) extracted from fibroblasts or RSC96 Schwann cells (magnification, x25,000). Scale bar, 200 nm. (B) Protein expression of exosome marker proteins CD81 and CD63, and the endoplasmic reticulum marker Calnexin were assessed by western blotting.

Table I. Primer sequences for reverse transcription-quantitative PCR.

| Gene | Primer sequence (5'→3') |
|---|---|
| S100 | F: GGTTGCCCTCATTGATGTCTTCC |
| | R: ACCACTTCCTGCTCTTTGATTTCC |
| Sox10 | F: GGGCAAGGTCAAGAAGGAACAG |
| | R: ACCAGCGTCCAGTCGTAGC |
| EGR2 | F: CTACCCCCTACAATCCGCAC |
| | R: GATTCGGATGTGCCTGGTCA |
| GFAP | F:CAAGAAACAGAAGAGTGGTATCGGT |
| | R: ACTCAAGGTCGCAGGTCAAGG |
| NGFR | F: CCTGCTGCTGCTGCTGATTC |
| | R: GTTCACACACGGTCTGGTTGG |
| GAPDH | F: TCAAGAAGGTGGTGAAGCAGG |
| | R: TCAAGAAGGTGGTGAAGCAGG |

EGR2, early growth response protein 2; GFAP, glial fibrillary acidic protein; NGFR, low-affinity nerve growth factor receptor.

anti-rabbit secondary antibody (1:5,000; cat. no. BA1054; Boster Biological Technology) for 2 h at 37˚C on a shaker. The membrane was thoroughly washed three times (10 min each) with 0.05% TBST. Protein bands were visualized using an ECL kit (CWBio), according to the manufacturer's protocol. Images of the membrane were captured using a chemiluminescence imager (ChemiDoc™ MP Imaging System; Bio-Rad Laboratories).

*Immunofluorescence assay*. BMSCs ($2x10^4$ cells/well) were seeded into 24-well plates; cells were divided into three groups, cultured with different media as described above, and collected after differentiation for 7 days. Following the removal of the culture media, cells were washed twice with PBS and fixed with 4% paraformaldehyde for 15 min at room temperature. Cells were washed three times with PBS and blocked with 1% BSA (CWBio) at 37˚C for 30 min and subsequently incubated with the following primary antibodies overnight at 4˚C: Anti-Sox10 (1:250), anti-EGR2 (1:100), anti-NGFR (1:50), anti-S100 (1:100) and anti-GFAP (1:100). Cells were washed three times with PBS for 5 min each and incubated with goat anti-rabbit IgG H&L (Alexa Fluor® 488; 1:500; cat. no. ab150077; Abcam) at 37˚C for 30 min. The cells were washed three times with PBS for 5 min each and incubated at room temperature with DAPI for 5 min in the dark. The plate was mounted with the Fluoromount-G® blocking solution containing anti-fluorescence quencher (cat. no. 0100-01; SouthernBiotech). Cells were visualized using an Olympus BX53 fluorescence microscope (magnification, x100; Olympus Corporation). To calculate the positive rate: 5 fields were randomly selected in each plate, all cells were counted and the expression rate of positive cells was calculated.

*Statistical analysis*. Statistical analysis was performed using SPSS version 17.2 (SPSS, Inc.) software. The data was presented as the mean ± SD; n=3. RT-qPCR, western blotting and immunofluorescence results were analyzed using one-way ANOVA followed by Newman-Keuls Multiple Comparison test. $P<0.05$ was considered to indicate a statistically significant difference.

## Results

*Exosome extraction, isolation and identification*. Schwann cell- and fibroblast-derived exosomes were visualized using TEM. Observed exosomes presented as irregular discoid vesicles with a diameter of ~50-80 nm (Fig. 1A). The concentration of protein extracted from the exosomes of RSC96 cells and fibroblasts was 1.22 and 1.10 $\mu g/\mu l$, respectively. The exosomal marker proteins CD81 and CD63 were detected by western blotting in both RSC96 cells and fibroblasts, whereas the endoplasmic reticulum marker protein Calnexin was not detected (Fig. 1B). Overall, this indicated that exosomes were successfully extracted from RSC96 cells and fibroblasts.

*Cell morphology of BMSCs*. The differentiation of BMSCs was induced according to the experimental design

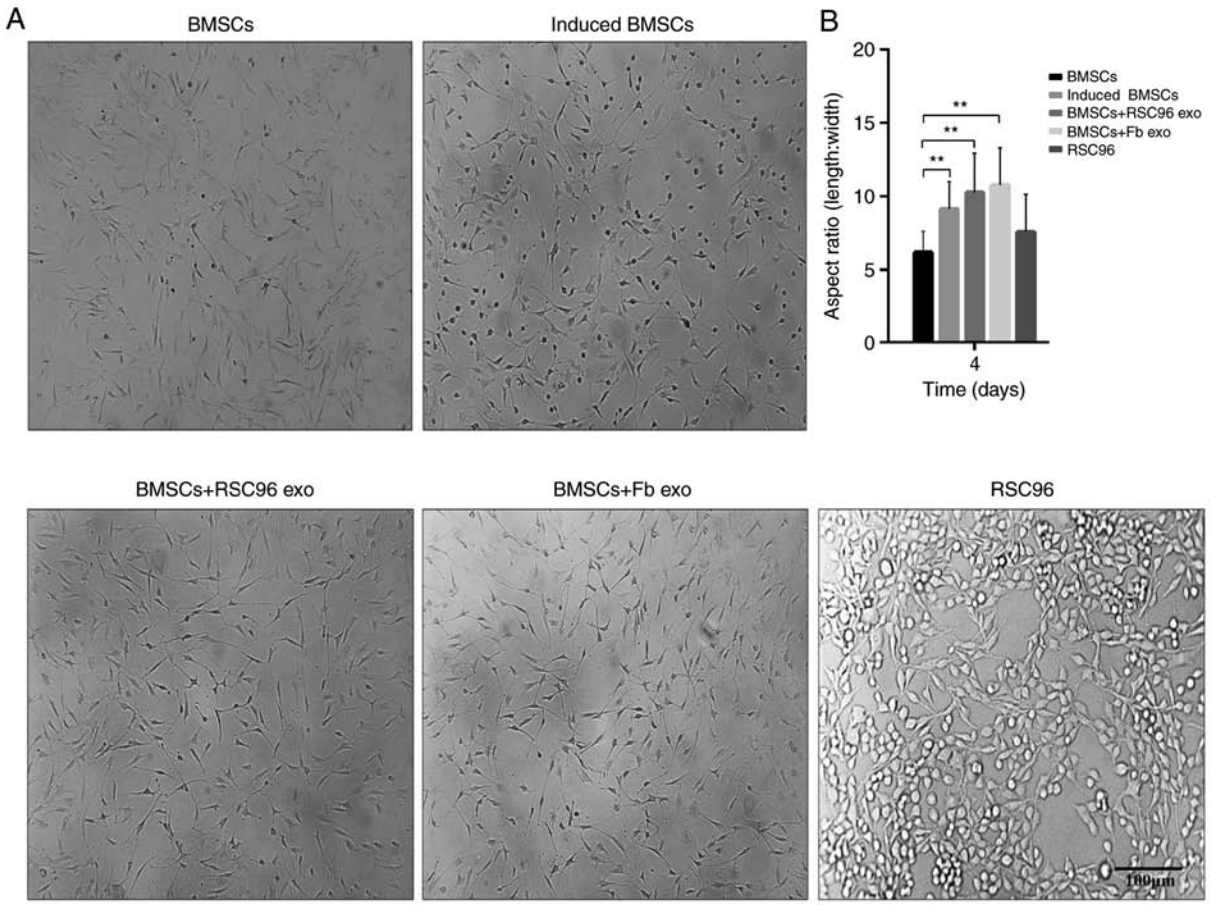


Figure 2. Cell morphology of BMSCs. (A) Cell morphology of control BMSCs, induced BMSCs, BMSCs + RSC96 exo, BMSCs + Fb exo or RSC96 cells after 4 days of induction (magnification, x200). Scale bar, 100 $\mu$m. (B) Quantitative analysis of the BMSC length/width ratio. $^{**}$P<0.01. BMSCs, bone marrow-derived mesenchymal stem cells; Fb ex, fibroblast-derived exosomes; induced BMSCs, Dezawa's induction method; RSC96 exo, Schwann cell-derived exosomes.

aforementioned, and the morphological features of BMSCs were evaluated 4 days post-induction. The morphology of BMSCs gradually changed from fibroblast-like morphology to a more fusiform shape, and the length/width ratio significantly increased in induced BMSCs compared with control BCSCs (Fig. 2A and B). Following the addition of Schwann cell- or fibroblast-derived exosomes to the cultured BMSCs, the length/width ratio of the BMSCs in these two groups (BMSCs + RSC96 exo and BMSCs + Fb exo, respectively) significantly increased compared with control BMSCs (Fig. 2A and B); however, there was no significant difference in cell morphology between BMSCs + RSC96 exo and BMSCs + Fb exo (Fig. 2B).

*mRNA and protein expression levels of Schwann cell markers in BMSCs*. mRNA and protein expression levels of S100, GFAP, Sox10, NGFR and EGR2 in induced BMSCs were significantly increased compared with the control BMSCs (Fig. 3A-G). In addition, the expression levels of S100, GFAP, Sox10, NGFR and EGR2 in the BMSCs + RSC96 exo group were significantly increased compared with control BMSCs and BMSCs + Fb exo groups (Fig. 3A-G); however, expression levels were not significantly different compared with induced BMSCs. The expression levels of Schwann cell markers in the BMSCs + Fb exo group were not significantly different compared with control BMSCs (Fig. 3A-G).

Results from immunofluorescence investigations demonstrated that the positive expression rates of S100, GFAP, NGFR, Sox10 and EGR2 were significantly increased in induced BMSCs compared with control BMSCs (Fig. 4); the expression levels of these Schwann cell markers were also significantly increased in the BMSCs + RSC96 exo group compared to the control BMSCs. In addition, the protein expression levels of all Schwann cell markers were significantly increased in the BMSCs + RSC96 exo group compared with the BMSCs + Fb exo group, which did not display significantly altered expression levels compared with control BMSCs (Fig. 4). This was consistent with the RT-qPCR and western blotting results (Fig. 3). These results suggested that Schwann cell-derived exosomes may promote the differentiation of BMSCs into Schwann cells because the expression levels of Schwann cell marker proteins and transcription factors increased following the induction, whereas fibroblast-derived exosomes were not observed to promote the same function.

## Discussion

Results from the present study demonstrated that Schwann cell-derived exosomes may induce BMSCs to differentiate into Schwann cells. During induction, BMSCs express Schwann cell surface markers at multiple developmental stages; these include S100, GFAP, NGRF, Sox10 and

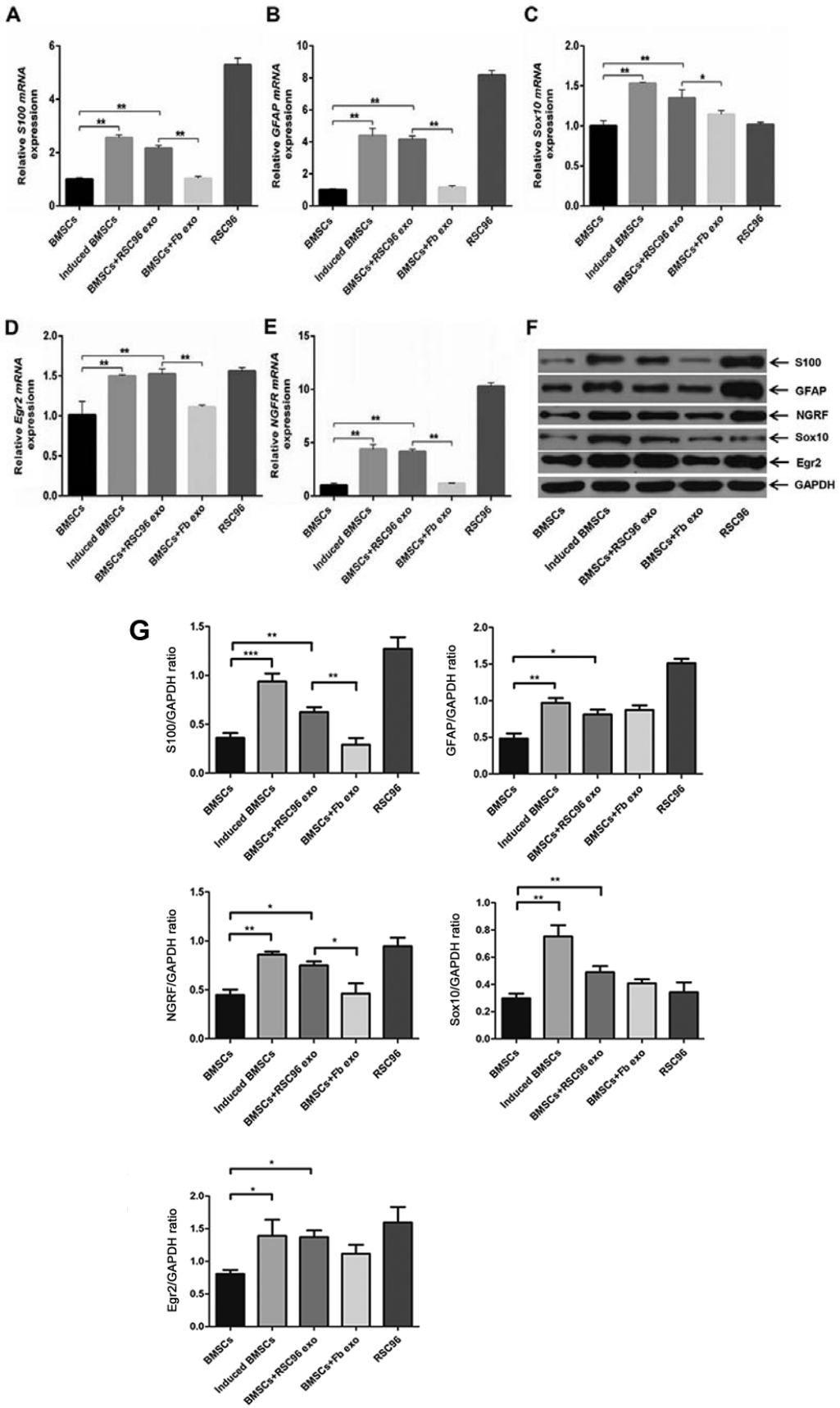


Figure 3. mRNA and protein expression levels of Schwann cell markers in differentially-induced BMSCs. (A-E) mRNA expression levels of (A) S100, (B) GFAP, (C) Sox10, (D) EGR2 and (E) NGFR in control BMSCs, induced BMSCs, BMSCs + RSC96 exo, BMSCs + Fb exo or RSC96 cells. (F and G) Representative immunoblot of protein expression levels of S100, GFAP, NGRF, Sox10, EGR2 and GAPDH in control BMSCs, induced BMSCs, BMSCs + RSC96 exo, BMSCs + Fb exo or RSC96 cells. Data are presented as mean ± SD; $^{*}$P<0.05, $^{**}$P<0.01 and $^{***}$P<0.001. BMSCs, bone marrow mesenchymal stem cells; EGR2, early growth response 2; Fb exo, fibroblast-derived exosomes; GFAP, glial fibrillary acidic protein; induced BMSCs, Dezawa's induction method; NGFR, low-affinity nerve growth factor receptor; RSC96 exo, Schwann cell-derived exosomes.

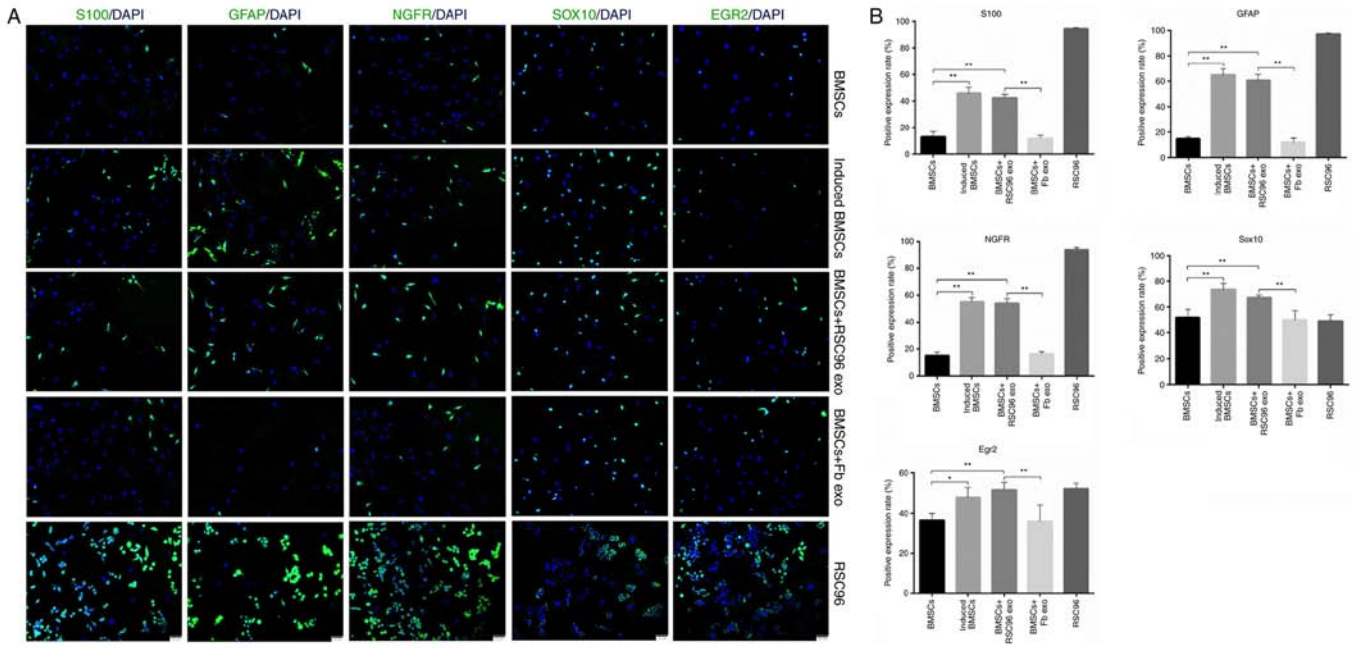


Figure 4. Protein expression of Schwann cell markers in differentially-induced BMSCs. (A) Representative immunofluorescence micrographs of Schwann cell-associated marker expressions (S100, GFAP, NGRF, Sox10 and EGR2) in control BMSCs, induced BMSCs, BMSCs + RSC96 exo, BMSCs + Fb exo or RSC96 cells (magnification, x100). Scale bar, 50 $\mu$m. (B) Quantitative analysis of the expression of Schwann cell-associated markers from (A) Data are presented as mean ± SD; $^{*}$P<0.05 and $^{**}$P<0.01. BMSCs, bone marrow mesenchymal stem cells; EGR2, early growth response 2; Fb exo, fibroblast-derived exosomes; GFAP, glial fibrillary acidic protein; induced BMSCs, Dezawa's induction method; NGFR, low-affinity nerve growth factor receptor; RSC96 exo, Schwann cell-derived exosomes.

EGR2 (17-19). Sox10 and EGR2 are transcription factors that serve crucial roles in Schwann cell differentiation (20,21); Sox10 is expressed in neural crest cells and is required for the Schwann cell phenotype and progression beyond the immature stage (20); EGR2 is closely related to the differentiation of myelinating Schwann cells (21). Exosomes derived from fibroblasts were not observed to have increased expression levels of these markers, indicating that Schwann cell-derived exosomes may be widely involved in the differentiation of stem cells into Schwann cells.

Previous studies have used stem cell-induced differentiation with diverse induction methods to obtain Schwann-like cells, including the use of cytokines (3,22) and small molecule chemical reprogramming induction (23). BMSCS can differentiate and participate in nerve regeneration at lesion sites (3,22,23), suggesting that there might be a natural *in vivo* stem cell induction mechanism; however, this mechanism remains relatively unknown. Currently, the most accepted hypothesis is that BMSCs can differentiate into Schwann cells under the control of cytokines in the local microenvironment, which enables the newly differentiated Schwann cells to secrete corresponding neuronal factors that promote nerve regeneration or directly participate in the regeneration of the myelin sheath (24,25). It is also hypothesized that BMSCs can interact with local cells instead of differentiating into Schwann cells to promote these functions (26). However, to the best of our knowledge, previous studies have not investigated whether exosomes serve a role in the induction process. Our previous study reported that degenerative nerve distal tissue fluid may promote the differentiation of BMSCs into Schwann cells following nerve injury (15), suggesting that the source of the induced components in the microenvironment following nerve damage may be related to Wallerian degeneration. The present study demonstrated that exosomes derived from Schwann cells may be involved in the differentiation of BMSCs into Schwann cells. These results led to the hypothesis that exosomes may induce the differentiation of BMSCs into Schwann cells in a similar manner to cytokines, through interacting with microRNAs, mRNAs and proteins in the exosomes. Moreover, exosomes may also serve an important role in multiple developmental stages of Schwann cells.

The underlying mechanisms behind exosome-induced differentiation of BMSCs into Schwann cells remains unclear and further investigations are required; transcriptome sequencing and analysis may reveal the differences in the transcriptional profiles of BMSC-derived Schwann cells and Schwann cells. In addition, Schwann cell-derived exosomes are complex and versatile, but most research on exosomes focuses on their role in nerve regeneration (10,27-30). The exosomes produced by the newly dedifferentiated Schwann cells following nerve injury may differ from the exosomes derived from normal Schwann cells under healthy physiological conditions. Therefore, their function regarding the induction of Schwann cell differentiation needs to be further investigated. In addition, it could be that the exosome purity can affect MSCs induction, thus the failure to evaluate the exosome purity may impact the accuracy of the conclusions drawn from this study. In conclusion, the present study suggested that the role of exosomes in the differentiation of BMSCs into Schwann cells may represent a novel target for neural regeneration; however, these results were not validated in *in vivo* studies; thus, the efficiency of this induction method requires further study.

**Acknowledgements**

Not applicable.

**Funding**

This study was supported by The National Natural Science Foundation of China (grant. no. 81470682).

**Availability of data and materials**

The datasets used and/or analyzed during the current study are available from the corresponding author on reasonable request.

**Authors' contributions**

HW and YJ designed and performed the research. HW, YJ, JL and QL analyzed the data and were involved in writing the manuscript. All authors read and approved the final manuscript.

**Ethics approval and consent to participate**

All animal procedures were conducted in accordance with The Guidelines for Ethical Conduct in the Care and Use of Animals of the Chinese National Health and Medical Research Council, and were approved by the Animal Experimentation Ethics Committee of Capital Medical College (Beijing, China; protocol no. AEEI-2016-135).

**Patient consent for publication**

Not applicable.

**Competing interests**

The authors declare that they have no competing interests.

**References**

1. Chen X, Wang XD, Chen G, Lin WW, Yao J and Gu XS: Study of in vivo differentiation of rat bone marrow stromal cells into Schwann cell-like cells. Microsurgery 26: 111-115, 2006.
2. Cuevas P, Carceller F, Dujovny M, Garcia-Gómez I, Cuevas B, González-Corrochano R, Diaz-González D and Reimers D: Peripheral nerve regeneration by bone marrow stromal cells. Neurol Res 24: 634-638, 2002.
3. Dezawa M, Takahashi I, Esaki M, Takano M and Sawada H: Sciatic nerve regeneration in rats induced by transplantation of in vitro differentiated bone-marrow stromal cells. Eur J Neurosci 14: 1771-1776, 2001.
4. Ladak A, Olson J, Tredget EE and Gordon T: Differentiation of mesenchymal stem cells to support peripheral nerve regeneration in a rat model. Exp Neurol 228: 242-252, 2011.
5. Shen J, Duan XH, Cheng LN, Zhong XM, Guo RM, Zhang F, Zhou CP and Liang BL: In vivo MR imaging tracking of transplanted mesenchymal stem cells in a rabbit model of acute peripheral nerve traction injury. J Magn Reson Imaging 32: 1076-1085, 2010.
6. Tohill M, Mantovani C, Wiberg M and Terenghi G: Rat bone marrow mesenchymal stem cells express glial markers and stimulate nerve regeneration. Neurosci Lett 362: 200-203, 2004.
7. Keller S, Sanderson MP, Stoeck A and Altevogt P: Exosomes: From biogenesis and secretion to biological function. Immunol Lett 107: 102-108, 2006.
8. van der Pol E, Boing AN, Harrison P, Sturk A and Nieuwland R: Classification, functions, and clinical relevance of extracellular vesicles. Pharmacol Rev 64: 676-705, 2012.
9. van Niel G, Porto-Carreiro I, Simoes S and Raposo G: Exosomes: A common pathway for a specialized function. J Biochem 140: 13-21, 2006.
10. Ching RC and Kingham PJ: The role of exosomes in peripheral nerve regeneration. Neural Regen Res 10: 743-747, 2015.
11. Lopez-Leal R and Court FA: Schwann cell exosomes mediate neuron-glia communication and enhance axonal regeneration. Cell Mol Neurobiol 36: 429-436, 2016.
12. Ravasi M, Scuteri A, Pasini S, Bossi M, Menendez VR, Maggioni D and Tredici G: Undifferentiated MSCs are able to myelinate DRG neuron processes through p75. Exp Cell Res 319: 2989-2999, 2013.
13. Zhu S, Li J, Zhu Q, Dai T, He B, Zhou X, Xiang J and Liu X: Differentiation of human amniotic epithelial cells into Schwann-like cells via indirect co-culture with Schwann cells *in vitro*. Mol Med Rep 11: 1221-1227, 2015.
14. Wei Y, Gong K, Zheng Z, Liu L, Wang A, Zhang L, Ao Q, Gong Y and Zhang X: Schwann-like cell differentiation of rat adipose-derived stem cells by indirect co-culture with Schwann cells in vitro. Cell Prolif 43: 606-616, 2010.
15. Wang H, Zhang H, Liu M and Wang N: Distal segment extracts of the degenerated rat sciatic nerve induce bone marrow stromal cells to express Schwann cell markers in vitro. Neurosci Lett 544: 89-93, 2013.
16. Livak KJ and Schmittgen TD: Analysis of relative gene expression data using quantitative PCR and the 2(-Delta Delta C(T)) method. Methods 25: 402-408, 2001.
17. Finzsch M, Schreiner S, Kichko T, Reeh P, Tamm ER, Bösl MR, Meijer D and Wegner M: Sox10 is required for Schwann cell identity and progression beyond the immature Schwann cell stage. J Cell Biol 189: 701-712, 2010.
18. Bremer M, Frob F, Kichko T, Reeh P, Tamm ER, Suter U and Wegner M: Sox10 is required for Schwann-cell homeostasis and myelin maintenance in the adult peripheral nerve. Glia 59: 1022-1032, 2011.
19. Jaegle M and Meijer D: Role of Oct-6 in Schwann cell differentiation. Microsc Res Tech 41: 372-378, 1998.
20. Britsch S, Goerich DE, Riethmacher D, Peirano RI, Rossner M, Nave KA, Birchmeier C and Wegner M: The transcription factor Sox10 is a key regulator of peripheral glial development. Genes Dev 15: 66-78, 2001.
21. Zorick TS, Syroid DE, Brown A, Gridley T and Lemke G: Krox-20 controls SCIP expression, cell cycle exit and susceptibility to apoptosis in developing myelinating Schwann cells. Development 126: 1397-1406, 1999.
22. Cai S, Tsui YP, Tam KW, Shea GK, Chang RS, Ao Q, Shum DK and Chan YS: Directed differentiation of human bone marrow stromal cells to fate-committed schwann cells. Stem Cell Reports 9: 1097-1108, 2017.
23. Thoma EC, Merkl C, Heckel T, Haab R, Knoflach F, Nowaczyk C, Flint N, Jagasia R, Jensen Zoffmann S, Truong HH, *et al*: Chemical conversion of human fibroblasts into functional Schwann cells. Stem Cell Reports 3: 539-547, 2014.
24. Keilhoff G, Goihl A, Stang F, Wolf G and Fansa H: Peripheral nerve tissue engineering: Autologous Schwann cells vs. transdifferentiated mesenchymal stem cells. Tissue Eng 12: 1451-1465, 2006.
25. Choi BH, Zhu SJ, Kim BY, Huh JY, Lee SH and Jung JH: Transplantation of cultured bone marrow stromal cells to improve peripheral nerve regeneration. Int J Oral Maxillofac Surg 34: 537-542, 2005.
26. Weimann JM, Charlton CA, Brazelton TR, Hackman RC and Blau HM: Contribution of transplanted bone marrow cells to Purkinje neurons in human adult brains. Proc Natl Acad Sci USA 100: 2088-2093, 2003.
27. Lopez-Leal R, Alvarez J and Court FA: Origin of axonal proteins: Is the axon-schwann cell unit a functional syncytium? Cytoskeleton (Hoboken) 73: 629-639, 2016.
28. De Gregorio C, Diaz P, Lopez-Leal R, Manque P and Court FA: Purification of exosomes from primary Schwann cells, RNA extraction, and next-generation sequencing of exosomal RNAs. Methods Mol Biol 1739: 299-315, 2018.
29. Qing L, Chen H, Tang J and Jia X: Exosomes and their MicroRNA cargo: New players in peripheral nerve regeneration. Neurorehabil Neural Repair 32: 765-776, 2018.
30. Simeoli R, Montague K, Jones HR, Castaldi L, Chambers D, Kelleher JH, Vacca V, Pitcher T, Grist J, Al-Ahdal H, *et al*: Exosomal cargo including microRNA regulates sensory neuron to macrophage communication after nerve trauma. Nat Commun 8: 1778, 2017.